Available online at www.sciencedirect.com

ScienceDirect

Deep-Sea Research II 54 (2007) 2174–2190

DEEP-SEA RESEARCH
PART II

www.elsevier.com/locate/dsr2

The island mass effect and biological carbon uptake for the subantarctic Crozet Archipelago

Dorothee C.E. Bakker[a,*], Maria C. Nielsdóttir[a,b], Paul J. Morris[b], Hugh J. Venables[b], Andrew J. Watson[a]

[a]*School of Environmental Sciences, University of East Anglia, Norwich NR4 7TJ, UK*
[b]*National Oceanography Centre Southampton, Southampton SO14 3ZH, UK*

Received in revised form 7 June 2007; accepted 24 June 2007
Available online 21 September 2007

Abstract

Marine productivity is often higher downstream than upstream of islands. This so-called island mass effect was tested and quantified with respect to biological carbon uptake and air–sea exchange of carbon dioxide (CO_2) at the Crozet Plateau between November 2004 and January 2005 during two CROZEX cruises. The remote plateau is situated at 45.5–47.0°S 49.0–53.0°E, south of the Subantarctic Front (SAF) in the Polar Frontal Zone (PFZ). Surface waters upstream (south) of the plateau had high nutrient and low chlorophyll (HNLC) concentrations. The fugacity of carbon dioxide (fCO_2) in surface water was just below the atmospheric value and oceanic CO_2 uptake was small ($0.2 \pm 0.1\,mol\,m^{-2}$) throughout CROZEX. The mixed-layer concentration of dissolved inorganic carbon (DIC) decreased by $15\,\mu mol\,kg^{-1}$ from November to January in these HNLC waters, indicating significant biological carbon uptake. Extensive phytoplankton blooms occurred downstream (north) of the plateau in austral spring. These reduced surface water fCO_2 by 30–70 μatm and DIC by $30–60\,\mu mol\,kg^{-1}$ and created an important oceanic sink for atmospheric CO_2 of $0.6–0.8 \pm 0.4\,mol\,m^{-2}$, corresponding to a total uptake of $1.3 \pm 0.8\,Tg\,C$ ($1\,Tg = 10^{12}\,g$). The reduction of DIC in the upper 100 m was much larger downstream ($2–3\,mol\,m^{-2}$) than upstream ($1\,mol\,m^{-2}$) of the plateau in January, further confirming the existence of the island mass effect for the Crozet Archipelago. An additional finding is the sizeable DIC deficit in the HNLC waters upstream (south) of the plateau, suggesting that some HNLC waters of the PFZ are more productive than commonly thought. Deep mixed layers of 60–90 m may hide such sustained, modest marine productivity from detection by satellite.

Keywords: Carbon dioxide; Island mass effect; Iron supply

1. Introduction

The remote Polar Frontal Zone (PFZ), between the Subantarctic Front (SAF) and the Polar Front (PF) (Fig. 1A) (Pollard et al., 2002), is a frontier in marine carbon cycle research. Deep-ocean waters reach the surface south of the PF, travel northward across the PFZ, and leave the surface north of the SAF as Antarctic Intermediate Water (AAIW). The circumpolar PFZ is an important area for the exchange of heat, moisture and biogeochemical properties between the ocean and the atmosphere

*Corresponding author. Tel.: +44 1603 592648; fax: +44 1603 591327.
E-mail address: D.Bakker@uea.ac.uk (D.C.E. Bakker).

0967-0645/$ - see front matter © 2007 Elsevier Ltd. All rights reserved.
doi:10.1016/j.dsr2.2007.06.009

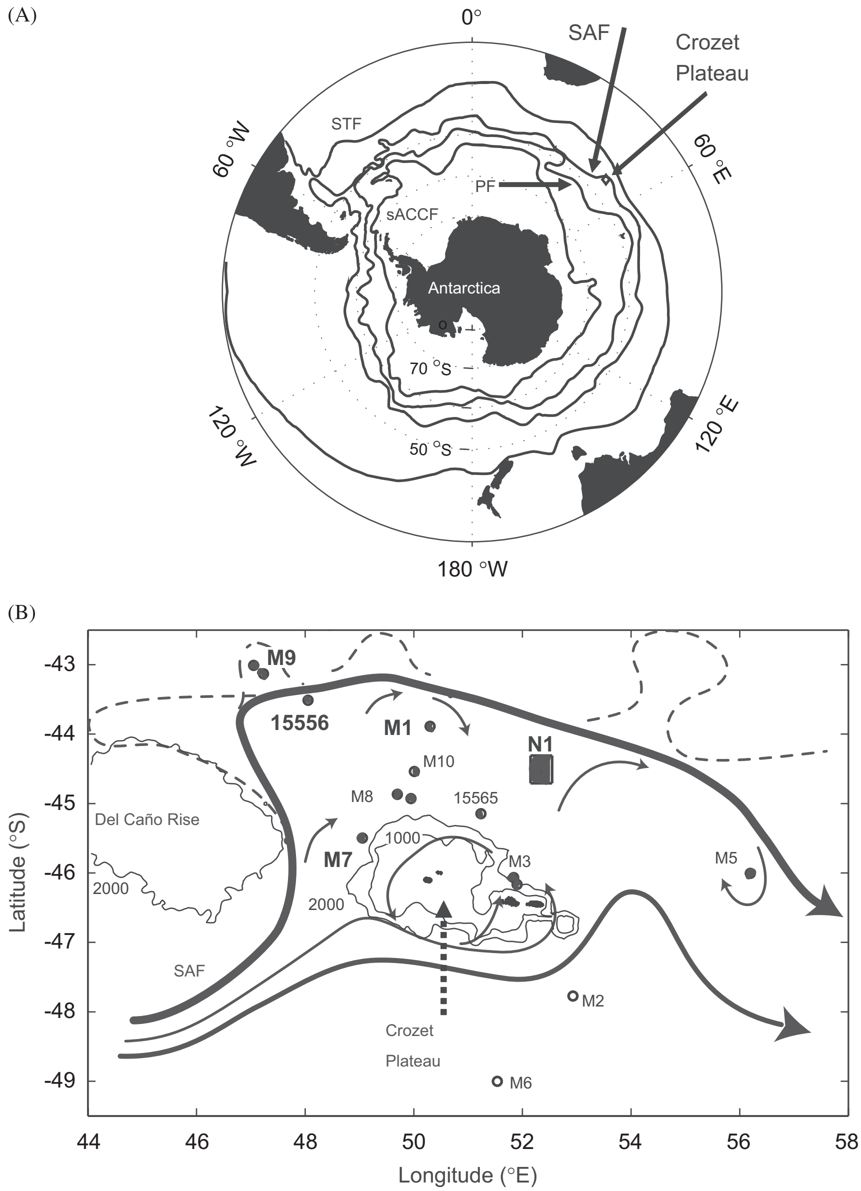

Fig. 1. (A, B) The Crozet Plateau is in the Polar Frontal Zone in a northward bend of the Subantarctic Front (SAF). (A) Other fronts are the Subtropical Front (STF), the Polar Front (PF) and the southern Front of the Antarctic Circumpolar Current (sACCF) (Orsi et al., 1995). (B) Arrows indicate currents in the Crozet area (from Pollard et al., 2007): the fast-flowing SAF (heavy line) with its large meanders (dashed lines); weak currents between the SAF and the plateau; anticyclonic flow around the plateau, and eastward flow south of the plateau. Circles correspond to stations upstream (south) (open circles) and downstream (edge, north, east) (closed circles) of the plateau (Table 1). The closed rectangle indicates area N1. The labels of highly productive sites are in bold. Depth contours are at 1000 and 2000 m (Smith and Sandwell, 1997).

(Speer et al., 2000; Rintoul et al., 2001). Fundamental uncertainties exist on the size of marine productivity, carbon export, uptake of atmospheric carbon dioxide (CO_2), and the storage of anthropogenic CO_2 in the PFZ and adjacent areas (Antoine et al., 1996; Banse, 1996; Behrenfeld and Falkowski, 1997; Rayner et al., 1999; Caldeira and Duffy, 2000; Moore and Abbott, 2000; Gurney et al., 2002; Schlitzer, 2002; Takahashi et al., 2002; Sabine et al., 2004; Lo Monaco et al., 2005; Peylin et al., 2005; Metzl et al., 2006). Undersampling of the marine carbon system is an important factor in the above uncertainties, in particular with high variability of biogeochemical properties in summer and low data availability in austral winter (Metzl et al., 2006).

Surface waters in the PFZ typically have high concentrations of nitrate and phosphate, while silicate concentrations become low during the growing season (Nelson et al., 2002; Pollard et al., 2002). Large parts of the PFZ have low phytoplankton growth (Banse, 1996). Purposeful iron fertilization experiments have demonstrated that low iron concentrations may limit phytoplankton growth in the high-nutrient low-chlorophyll (HNLC) waters of the PFZ (Gervais et al., 2002; Coale et al., 2004). Other factors, notably the amount of incoming solar irradiance, the mixed-layer depth, and grazing intensity may also limit phytoplankton growth (Nelson and Smith, 1991; Banse, 1996; Platt et al., 2003). Co-limitation of iron and light may occur at low light levels (Sunda and Huntsman, 1997; Boyd et al., 1999). Thus, a complex interplay of factors controls the timing and size of phytoplankton growth, inorganic carbon uptake, CO_2 air–sea exchange, and carbon export in the PFZ.

High marine productivity occurs near frontal systems and downstream of islands and shallow topography in the Antarctic Circumpolar Current (ACC) in austral summer (Sullivan et al., 1993; Moore and Abbott, 2002; Tyrrell et al., 2005). High iron concentrations have been found in spring blooms at the PF at 6°W, and it has been suggested that the iron originated from an upstream sediment source, potentially the Scotia Ridge or the Northeast Georgia Rise at 1600 km distance (De Baar et al., 1995; Korb et al., 2004). High iron concentrations downstream of the Kerguelen and Crozet Plateaus originated from shallow sediments on the plateaus (Bucciarelli et al., 2001; Planquette et al., 2007). The above observations indicate that natural iron sources fuel marine productivity downstream.

This study tests and quantifies the 'island mass effect', the occurrence of higher marine productivity downstream than upstream of an island (Doty and Oguri, 1956; Gilmartin and Revelante, 1974), with respect to the marine carbon cycle and CO_2 air–sea exchange at the Crozet Plateau. In the presence of an island mass effect, we expect higher biological carbon uptake and a stronger oceanic CO_2 sink (or a weaker oceanic CO_2 source) downstream than upstream of the plateau.

The study area, the waters upstream and downstream of the Crozet Plateau, is in the PFZ (Fig. 1A) (Pollard et al., 2002, 2007). The volcanic Crozet Plateau (45.5–47.0°S 49.0–53.0°E) is situated 2500 km southeast of South Africa and rises steeply out of the neighbouring, 3800 m deep ocean basins (Fig. 1B). Ile de la Possession and Ile de l'Est are islands on the eastern side of the plateau. The SAF passes northward between the Del Caño Rise and the Crozet Plateau before resuming its eastward flow ~250 km north of the plateau (Pollard and Reid, 2001; Pollard et al., 2007). Water south of the plateau at 47.5–49.0°S flows eastward and has not been influenced by the plateau. Surface waters in this region have high concentrations of the major nutrients, nitrate and phosphate, and chlorophyll *a* concentrations, as seen by satellite (Fig. 2) (Sanders et al., 2007; Sanders, personal communication; Venables et al., 2007). The waters upstream or south of the plateau meet the definition of HNLC waters.

Water moves anticlockwise around and over the Crozet Plateau (Fig. 1B). Small phytoplankton blooms develop on the edges of the plateau in most years, some as late as December and January (Fig. 2) (Venables et al., 2007).

Extensive seasonal phytoplankton blooms occur every year north of the plateau (Fig. 2) (Venables et al., 2007). The blooms develop from September to October, peak in October–November, and decline afterwards. Low chlorophyll *a* concentrations in the SAF form the western and northern limits of the blooms (Venables et al., 2007). Currents in the bloom area are weak and water resides here for approximately 60 days (Pollard et al., 2007). A substantial fraction of the waters north of the plateau has passed over or along the plateau, such that these waters are downstream of the plateau. Low chlorophyll waters enter the bloom area from the SAF by detrainment and from the south by anticyclonic flow around the plateau (Figs. 1B and 2) (Pollard et al., 2007; Venables et al., 2007).

Mixed-layer depths are deeper south than north of the plateau throughout the year, as indicated by Argo floats (Venables et al., 2007). Winter mixing depths vary from 100 to 250 m south of the plateau and from 75 to 150 m to its north. Summertime mixed-layer depths are 40–100 m south of the plateau and mostly less than 60 m north of it (Venables et al., 2007).

This study uses shipboard measurements for the quantification of the island mass effect on the cycling of dissolved inorganic carbon (DIC) and CO_2 air–sea transfer in the vicinity of the Crozet

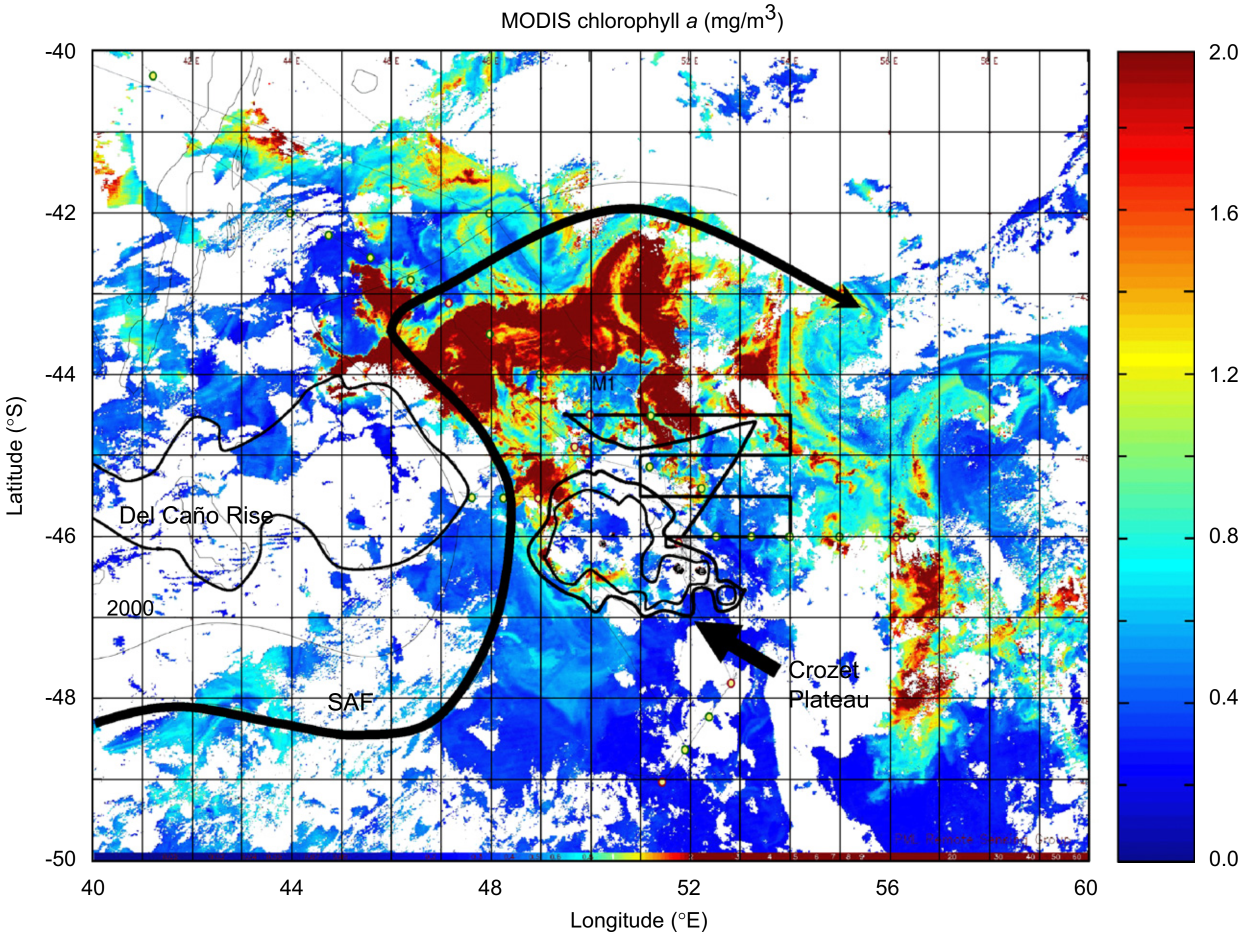

Fig. 2. Surface-water chlorophyll *a* (mg m^{-3}) for 14–18 November 2004 from the MODIS satellite. This real-time image has the highest resolution at 1 km × 1 km available for the Crozet area. The zigzag line corresponds to the ship's track from 10 to 18 November. The thick arrow indicates the approximate position of the Subantarctic Front (SAF) (after Pollard and Reid, 2001). Depth contours are at 1000 and 2000 m (curved lines) (Smith and Sandwell, 1997). The image is courtesy of the National Aeronautics and Space Administration (NASA) and the Remote Sensing Data Analysis Service (RSDAS).

Plateau. The data were collected during two CROZEX (CROZet natural iron bloom and EXport experiment) cruises on *RRS Discovery* from 3 November to 10 December 2004 (D285) and from 13 December 2004 to 21 January 2005 (D286). Observations upstream (south) (stations M2, M6) of the Crozet Plateau are contrasted to those downstream of the plateau in Sections 3.1 and 3.2 (Fig. 1B; Table 1). The area downstream is separated into waters on the edge (station M3), north (stations M1, M7, M8, M9, 15556, M10, 15565), and east (station M5) of the plateau. Oxygen (O_2) is used as an additional parameter. Surface waters are typically supersaturated by a few percent with O_2, as a result of bubbles injected into the water (Broecker and Peng, 1982). High primary productivity increases the O_2 saturation above this level.

2. Methods

2.1. Sampling during the CROZEX cruises

The position and timing of the stations are in Table 1 (Fig. 1B). Decimals indicate repeat occupations of the key stations in CROZEX, e.g. M3.1, M3.2, etc. Areas of 0.4° latitude by 0.4° longitude have been selected around the stations for averaging of surface water data (Table 1).

The ship's seawater supply collected large volumes of water from 5 m depth. Water from this supply was used for the continuous analysis of

Table 1
The position, timing and mixed layer depth (MLD) of the CROZEX stations (Fig. 1B), as well as the location of areas of 0.4° longitude by 0.4° latitude around the stations

	Code in text	Station	Date	Latitude (°S)	Longitude (°E)	MLD (m)	Latitude box (°S)	Longitude box (°E)
South	M2.1	15504	20/11/2004	−47.77	52.88	133	−48.0/−47.6	52.7/53.1
	M2.2	15606	07/01/2005	−47.80	52.85	63	−48.0/−47.6	52.7/53.1
	M6.1	15507	21/11/2004	−49.00	51.49	140	−49.2/−48.8	51.3/51.7
	M6.2	15596	03/01/2005	−49.00	51.53	93	−49.2/−48.8	51.3/51.7
Edge	M3.1	15494	13/11/2004	−46.06	51.79	11	−46.3/−45.9	51.7/52.1
	M3.2	15498	18/11/2004	−46.05	51.79	75	−46.3/−45.9	51.7/52.1
	M3.5	15589	31/12/2004	−46.07	51.78	60	−46.3/−45.9	51.7/52.1
	M3.6	15614	09/01/2005	−46.16	51.85	28	−46.3/−45.9	51.7/52.1
East	M5	15582	27/12/2004	−46.00	56.15	104	None	None
P-North	M8East	15532	30/11/2004	−44.92	49.90	59	None	None
	M8West	15538	02/12/2004	−44.86	49.65	45	None	None
	M10.1	15562	20/12/2004	−44.53	49.96	19	−44.7/−44.3	49.8/50.2
	M10.2	15632	15/01/2005	−44.50	49.99	28	−44.7/−44.3	49.8/50.2
	15565	15565	21/12/2004	−45.14	51.19	n.d.	−45.3/−44.9	51.0/51.4
HP-North	M1	15490	11/11/2004	−43.88	50.25	85	−44.1/−43.7	50.0/50.4
	N1	None	16/11/2004	None	None	None	−44.7/−44.3	52.1/52.5
	M7	15525	27/11/2004	−45.49	49.00	79	−45.7/−45.3	48.8/49.2
	M9.1	15544	04/12/2004	−43.12	47.18	48	−43.3/−42.9	46.9/47.3
	M9.2	15553	19/12/2004	−43.00	47.00	22	−43.3/−42.9	46.9/47.3
	15556	15556	19/12/2004	−43.50	48.00	n.d.	−43.7/−43.3	47.8/48.2

n.d. indicates that a value has not been determined.

temperature, salinity, the fugacity of CO_2 (fCO_2), the O_2 concentration, and for discrete sampling of DIC. Regular casts from the CTD rosette provided seawater for the analysis of DIC and O_2. Wind speed, atmospheric pressure and air temperature were determined by sensors at 18 m height and were reported at 10-min intervals. Wind speed and atmospheric pressure were corrected to 10 m above sea level (Large and Pond, 1981) and to sea level (Weiss and Price, 1980), respectively. Marine air was collected from an air inlet at the ship's 'monkey island'. The cruise data are stored at the British Oceanographic Data Centre (http://www.bodc.ac.uk/). Inorganic carbon and oxygen data are also in the CARBOOCEAN data base (http://www.carboocean.org).

The mixed-layer depth is defined here as the depth where the density exceeds that at 10 m depth by 0.05 kg m^{-3} (after Brainerd and Gregg, 1995; Venables et al., 2007). This definition provides an instantaneous value, which is between the depths of the actively mixed layer and the seasonal mixed layer. The mixed-layer depth has been calculated from 2 dbar depth profiles of salinity and temperature.

2.2. *The fugacity of CO_2 in surface water and marine air*

Measurements of fCO_2 in surface water and marine air were made by infrared detection with a system developed by Schuster and Watson (2007) and a fast-response equilibrator (Bakker et al., 2001). Mixing ratios of CO_2 and moisture were detected in the equilibrator headspace (every minute), in marine air (every 6 h), and in two secondary standards (every 6 h). The measurements were made with a continuous gas flow across an infrared LI-COR 6262. No difference in CO_2 readings was observed for flow and no flow conditions. Samples from the equilibrator headspace and marine air were partly dried before analysis. The first set of secondary standards had mixing ratios of 266.5 ± 0.1 and 481.1 ± 0.2 μmol CO_2 mol^{-1}; the second set of 267.8 ± 0.3 and 479.7 ± 0.3 μmol CO_2 mol^{-1}. These secondary standards were calibrated against certified NOAA standards before and after the cruises. Warming of the water between the seawater intake and the equilibrator was on average 0.4 °C ($\sigma = 0.1$ °C; 10,000 data points). The equation by Takahashi et al. (1993) was used to correct fCO_2 in seawater for this warming. The time delay between sampling and analysis was 1 min for fCO_2 in air and water. The precision and accuracy of the fCO_2 data was 1.0 μatm (Bakker et al., 2001).

Air–sea fluxes of CO_2 were calculated from fCO_2 in water and marine air and the 10-min shipboard wind speed at 10 m height. The equation of Wanninkhof (1992) for short-term shipboard wind speed was used.

2.3. The dissolved inorganic carbon concentration

Samples for DIC were collected in 500-ml glass bottles from the CTD rosette and the surface water supply. Typically six samples were collected in the upper 100 m, and three samples between 100 and 200 m. Most analyses were made within 1 day of collection, the remainder within 6 days. Upon sampling, 100 μl of a saturated mercuric chloride solution were added to samples that were not analysed within 24 h. Samples were stored in the dark at 5 °C before analysis. The DIC concentration was determined by coulometric analysis (Johnson et al., 1987). Three or more replicate analyses were made on each glass bottle. At least one certified reference material (CRM) from batches 65 and 66 (DOE, 1994) was used per coulometric cell and per CTD cast. The precision is taken as 1.3 μmol kg^{-1} from the maximum difference in DIC between replicate surface water samples. The accuracy is estimated as better than 2.0 μmol kg^{-1}.

2.4. The oxygen concentration in surface water

The O_2 concentration of surface water was measured every minute with an Aanderaa optode 3930 positioned in the continuous seawater supply. The O_2 concentration in seawater was calculated from the raw optode signal, calibration coefficients and equations in the manual (Aanderaa, 2003). Oxygen concentrations determined by Winkler titration (Williams et al., 2004) in CTD samples from the upper 15 m exceeded those from the optode by 10–20 μM according to this relationship:
$[O_2]_{Winkler} = [O_2]_{optode} + 0.22\,T^2 - 4.01\,T + 30.98$
(37 data points, root mean square error = 1.3 μM) for temperature (T). The equation was used for calibration of the optode values. The O_2 saturation of surface water was calculated from the corrected O_2 concentrations with equations by Garcia and Gordon (1992).

3. Results

3.1. Carbon uptake upstream of the Crozet Plateau

Marine productivity and inorganic carbon cycling are described for sites upstream (south) and downstream (on the edge, north, east) of the Crozet Plateau for November 2004 to January 2005 (Sections 3.1 and 3.2). Subsequently, CO_2 air–sea transfer and inorganic carbon uptake are quantified for both sides of the plateau (Section 3.3). The occurrence of an island mass effect is discussed afterwards (Section 4.1).

Upstream (south) of the plateau, the surface water chlorophyll *a* concentrations were mostly below 0.5 mg m^{-3} from September 2004 to January 2005, as seen in satellite observations and confirmed by shipboard measurements (Fig. 2) (Seeyave et al., 2007; Venables et al., 2007). Chlorophyll *a* concentrations were up to 0.8 mg m^{-3} in a mesoscale structure in mid-November south of the plateau (Fig. 2). The waters in the feature had probably been influenced by the plateau, since the SAF typically had low chlorophyll *a* concentrations (Venables et al., 2007).

Surface water fCO_2 was slightly below its atmospheric value south of the plateau in late November (Figs. 3–5). Six weeks later, ΔfCO_2(w−a) (the difference between fCO_2 in water and air) and DIC had decreased by 13 μatm and 15 μmol kg^{-1}, respectively, while the O_2 saturation had increased by a few percent (Figs. 5 and 6). The reduction in ΔfCO_2(w−a) would have been larger by 24 μatm, if surface water warming of 1.5 °C had not counteracted the change (Fig. 5).

3.2. Biological carbon uptake downstream of the Crozet Plateau

3.2.1. Productive waters north of the plateau

Extensive phytoplankton blooms developed south of the SAF and at some distance north (downstream) of the Crozet Plateau from late September 2004 onwards, as shown by ocean colour images from the MODIS satellite (Venables et al., 2007). The blooms gradually extended southwards towards the plateau, reaching their maximum intensity and extent in late October and decreasing in size until early December (Venables et al., 2007). The *RRS Discovery* reached the Crozet Archipelago in mid-November, shortly after the maximum extent of these blooms.

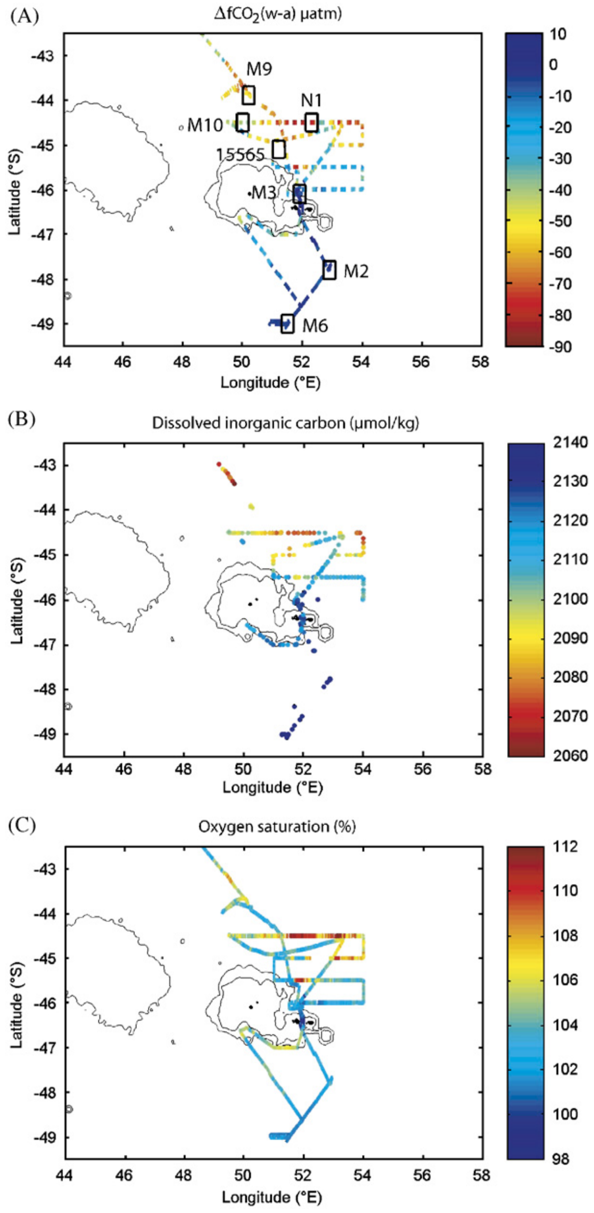

Fig. 3. (A) The difference of fCO_2 between surface water and air, ΔfCO_2(w−a), (B) DIC in surface water, and (C) the oxygen saturation near the Crozet Plateau between 8 and 24 November 2004. Depth contours are at 1000 and 2000 m (Smith and Sandwell, 1997).

The ship surveyed an area with high and low chlorophyll *a* concentrations north of the Crozet Plateau from 10 to 18 November (Fig. 2). Phytoplankton growth had locally decreased ΔfCO_2(w−a) by 70 µatm and DIC by 60 µmol kg^{-1} and had increased the O_2 saturation by 8% relative to nearby waters with a lower chlorophyll *a* concentration (Fig. 3). The reduction in ΔfCO_2(w−a) and DIC were largest at some distance north of the plateau (sites M1, N1), in the area with the earliest, longest lived, and most active phytoplankton blooms (Figs. 2–4). The reductions decreased via an area with shorter lived, less intense blooms (stations M10, 15565) towards the plateau, reflecting a gradient in phytoplankton CO_2 uptake from the northernmost bloom area towards the plateau. Temperature was not a major factor in creating this spatial variation of ΔfCO_2(w−a), as indicated by ΔfCO_2(w−a) corrected to a constant temperature (not shown).

Intense phytoplankton growth had strongly reduced ΔfCO_2(w−a) and DIC at station M7 on the northwestern side of the plateau in late November (Figs. 1B and 5). Biological carbon uptake was as large at M7 as at the most productive bloom sites north of the plateau (M1, N1). Two stations, M8West and M8East, which were 20 km apart, showed striking differences in primary productivity (Seeyave et al., 2007) and ΔfCO_2(w−a), thus highlighting the high spatial variability in the bloom area.

By late December, the bloom signature had largely disappeared in satellite chlorophyll *a* and ΔfCO_2(w−a) (Figs. 4 and 5) (Venables et al., 2007). The increase in ΔfCO_2(w−a) of 0–40 µatm had mainly resulted from surface water warming by 0.2–2.0 °C (corresponding to a change of 3–32 µatm) and CO_2 air–sea exchange. North of 45°S surface water warming continued from December to January (2.4 °C), resulting in a further increase of ΔfCO_2(w−a) (Fig. 4).

Arbitrarily we henceforth describe the highly productive northerly sites as HP-north (M1, N1, M7) and the productive sites as P-north (M10, M8West, M8East) with a continuum of algal carbon uptake between the two areas (Fig. 1B; Table 1). The small number of repeat visits to the productive and highly productive regions complicates a time series of events in these waters during CROZEX. The two most northerly stations (M9, 15556) were close to the strongly meandering SAF, in an area with strong spatial variability (Fig. 1B). Vertical salinity profiles indicate that these two stations were south of the SAF during site visits. Spatial variability may have exceeded temporal variability at these two stations.

3.2.2. *Local phytoplankton blooms on the edges of the plateau*

Local phytoplankton booms promoted algal carbon uptake on the edges of the Crozet Plateau.

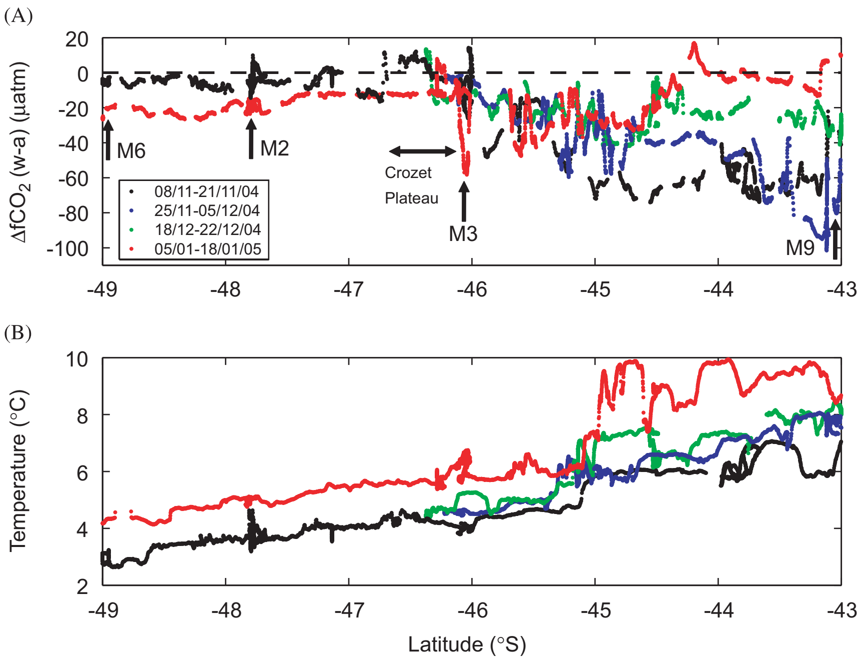

Fig. 4. (A) The difference of fCO_2 between surface water and air, ΔfCO_2(w−a), and (B) sea surface temperature along the ship's track, roughly from stations M6 via M2 and M3 to M9. The parameters are shown for four different passages of the ship. The cruise track varied between passages.

For example, a band with satellite chlorophyll *a* concentrations of 2 mg m^{-3} and ΔfCO_2(w−a) of −40 µatm was observed on the plateau's southern edge in November (Figs. 2 and 3).

Station M3 on the northeastern edge of the plateau was visited repeatedly. Satellite chlorophyll *a* concentrations were low at M3 from September to December 2004 (Venables et al., 2007). The ΔfCO_2(w−a) was just below zero, while the O_2 saturation was 102% in November and December (Figs. 3 and 5).

Maxima in ΔfCO_2(w−a) and DIC, and minima in the O_2 saturation and sea surface temperature (SST) were observed at M3 on 18 November (Figs. 5 and 6). Similar reductions in SST (−0.5 °C) and the O_2 saturation (−5%), and an increase in ΔfCO_2(w−a) (+5 µatm) were occasionally encountered elsewhere in the immediate vicinity of the Crozet Plateau, e.g. north of Ile de la Possession (46.29°S 51.67°E) on 10 and 12 January. These phenomena, as well as an uplift of the isotherms by 50 m (J. Allen, personal communication), also were observed between the two eastern islands on 31 December. The reduction in SST and the O_2 saturation and the increase in ΔfCO_2(w−a) point to the presence of water with an origin below the mixed layer. We suggest that mixing on the plateau introduced subsurface water into the mixed layer and that some of this water had reached M3 on 18 November.

A highly productive bloom of small diatoms was present in a cyclonic eddy near M3 in early January (Seeyave et al., 2007). The bloom had low ΔfCO_2(w−a) (−60 µatm) and DIC and an O_2 saturation of 111% in a shallow mixed layer (Figs. 5 and 6; Table 1). Surface waters of the M3 bloom may well have been influenced by horizontal or vertical advection, as suggested by the increase in DIC below the mixed layer (Fig. 6). The significant changes in water mass composition at M3 during CROZEX make it difficult to ascribe temporal changes in biogeochemical parameters to *in situ* processes.

3.3. Air–sea CO_2 transfer and the DIC deficit for the Crozet Archipelago

Comparisons of CO_2 air–sea transfer and the DIC deficit in the upper water column upstream and downstream of the plateau provide tools for testing and quantifying the island mass effect for the Crozet Plateau. Air–sea exchange of CO_2 has been calculated along the ship's track from shipboard wind speed and the gas transfer relationship for short-term shipboard wind speed by Wanninkhof (1992).

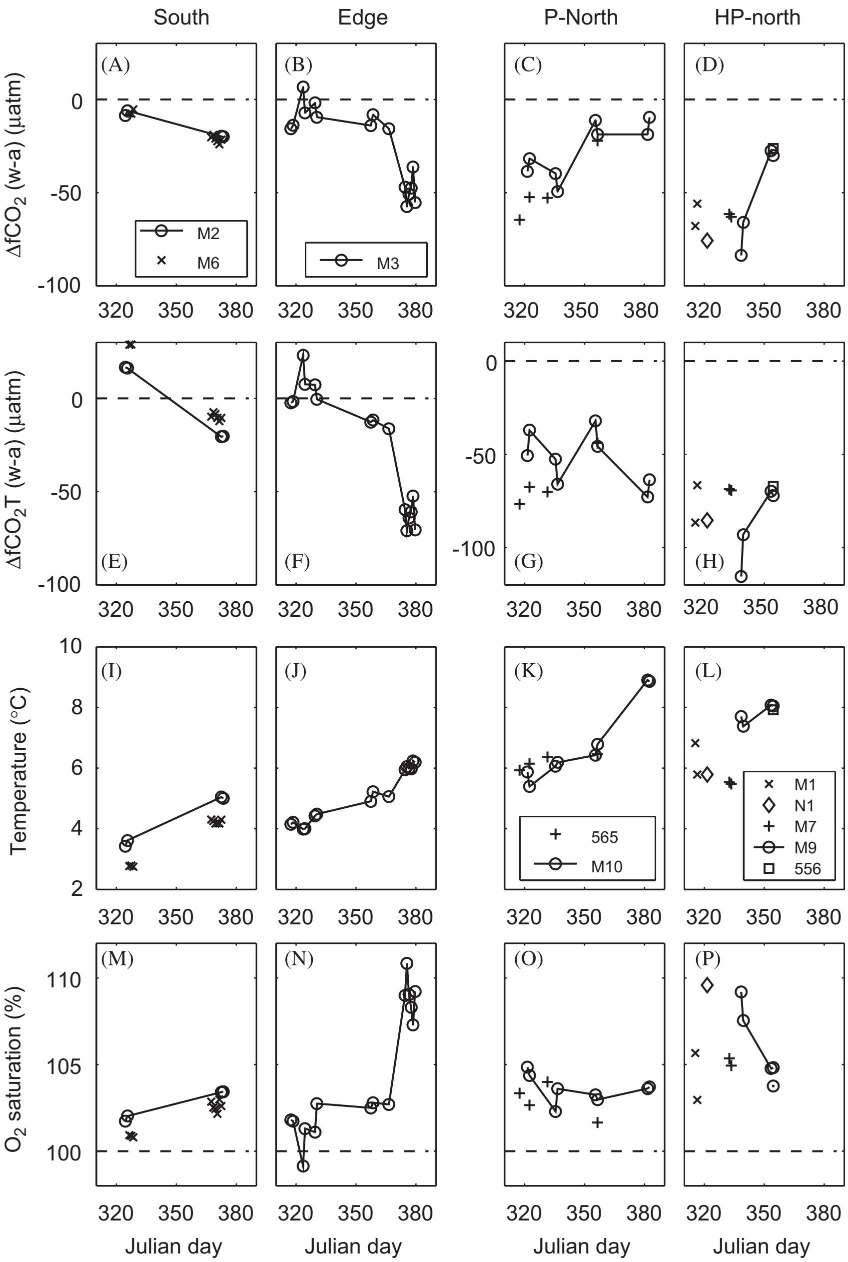

Fig. 5. Rows indicate, from top to bottom, (A–D) the difference of fCO_2 between surface water and marine air, (E–H) ΔfCO_2(w−a) normalized to 5.0 °C, (I–L) sea-surface temperature, and (M–P) the oxygen saturation in surface water for Julian days in 2004–2005. The columns correspond to, from left to right, areas of 0.4° latitude by 0.4° longitude south (upstream) of the plateau, on the edge of the plateau, and the productive (P) and highly productive (HP) regions north of the Crozet Plateau (Table 1). The figure legends are valid per column.

Average CO_2 air–sea fluxes upstream and downstream of the plateau have been calculated from daily averages for four periods, similar to those in Fig. 4 (Tables 2a and 2b).

Oceanic CO_2 uptake was low (on average 1–6 mmol m^{-2} d^{-1}) upstream (south) of the plateau throughout CROZEX (Table 2a). The bloom area north (downstream) of the plateau was a strong sink for atmospheric CO_2 (on average 9–24 mmol m^{-2} d^{-1}) in November, as a result of the undersaturation of surface water fCO_2 with respect to the atmospheric value. This oceanic CO_2 sink decreased

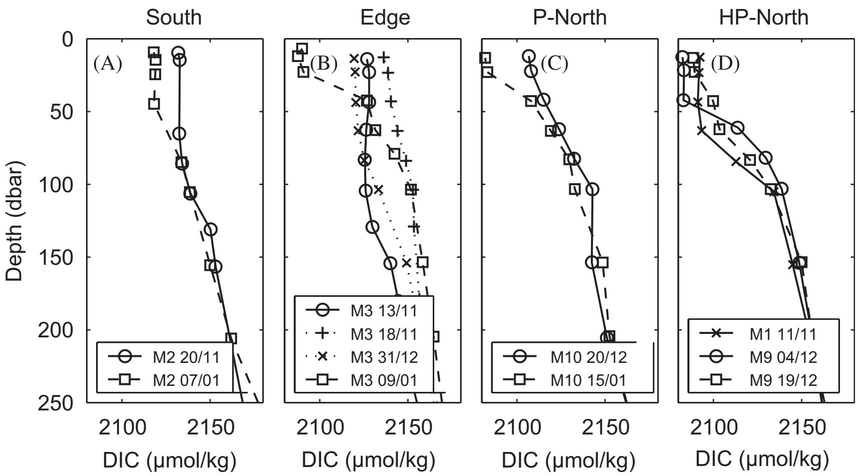

Fig. 6. The distribution of DIC in the upper 250 m for CTD stations (A) south (upstream) of, (B) on the edge of, (C) in the productive (P) north of, and (D) in the highly productive (HP) north of the Crozet Plateau. The position of the stations is in Table 1 and Fig. 1B.

Table 2a
Mean CO_2 air–sea fluxes and the standard deviation of the means for the regions in Table 2b during CROZEX

Period (length) Region	08/11–24/11 (17 d) Flux (mmol m^{-2} d^{-1})	25/11–04/12 (10 d) Flux (mmol m^{-2} d^{-1})	18/12–31/12 (14 d) Flux (mmol m^{-2} d^{-1})	01/01–16/01 (16 d) Flux (mmol m^{-2} d^{-1})	08/11–16/01 (75 d) Flux (mol m^{-2})	08/11–16/01 (75 d) Total flux (Tg C)
South	−1.2±0.8	n.d.	(−0.6±0.0)	−5.8±2.6	−0.24±0.12	−0.30±0.14
P-North	−9.2±9.1	−10.3±5.1	−4.4±3.4	−8.2±5.4	−0.58±0.42	−0.67±0.48
HP-North	−24.4±10.7	−11.5±6.6	−5.4±2.7	−2.2±0.6	−0.81±0.39	−0.65±0.31
Total						−1.62±0.93

The Wanninkhof relationship (1992) for short-term wind speed has been used. The fluxes have been calculated from daily flux averages along the cruise track. The periods are similar to those in Fig. 4. Tg C is 10^{12} g C. n.d. indicates that a value has not been determined.

Table 2b
Mean DIC deficit in the upper 100 m and the standard deviation of the mean at final visits to the stations in regions upstream and downstream of the Crozet Plateau

Region	Latitude (°S)	Longitude (°E)	Area (10^3 km^2)	DIC deficit (mol m^{-2})	Total DIC deficit (Tg C)
South	−49.0/−46.5	48.5/53.5	104	1.3±0.1	1.6±0.1
East	−46.5/−45.5	54.0/56.5	21	1.6±0.2	0.4±0.2
Edge	None	None	0	3.0±0.1	0
P-North	−46.5/−44.5	48.5/54.0	95	2.5±0.1	2.9±0.1
HP-North	−44.5/−43.0	47.0/52.0	67	3.4±0.2	2.7±0.1
Total			287	2.1±0.1	7.6±0.5

Tg C is 10^{12} g carbon.

in strength, as $\Delta f CO_2$(w−a) became less negative at the bloom stations in December. The average oceanic CO_2 sink downstream of the plateau was 0.6–0.8 mol m^{-2} during CROZEX, which corresponds to a sink for atmospheric CO_2 of 1.3±0.8 Tg C (1 Tg = 10^{12} g) (Table 2a).

The DIC deficit in the upper 100 m has been calculated from vertical DIC profiles relative to the

DIC concentration at 100 m depth. Vertical profiles have been obtained by interpolation at 0.1 m resolution between the DIC values. A 100 m depth range was chosen as mixed layers were shallower than 100 m north of the plateau, while no significant change in the DIC profiles was detected below 100 m at the southern stations during CROZEX (Fig. 6; Table 1). For consistency, the same depth is used for all stations. A 100 m depth range also has been used in other CROZEX and Southern Ocean studies (Table 3) (Sweeney et al., 2000; Bishop et al., 2004; Buesseler et al., 2004; Sanders et al., 2007).

The DIC deficit has been calculated for regions upstream and downstream of the Crozet Plateau by averaging the DIC deficit at final visits to the stations. The DIC deficit increased from upstream (south) ($1.3\pm0.1\,mol\,m^{-2}$) to downstream (north) (2.5–$3.4\,mol\,m^{-2}$) of the plateau (Fig. 7; Table 2b). The DIC deficit decreased further downstream, east of the plateau ($1.6\pm0.2\,mol\,m^{-2}$). Addition of the DIC deficit in each region provides a total DIC deficit in the Crozet area of 7.6 ± 0.5 Tg C.

Air–sea gas transfer supplied 0.6–0.8 mol C m^{-2} to the mixed layer of the main bloom area over 75 days, or 23–24% of the DIC deficit in January (Tables 2a and 2b). This resupply of DIC by air–sea gas exchange is slightly higher than observations in other actively growing Southern Ocean blooms,

Table 3
The mixed layer depth (MLD), average changes in fCO_2 across the air–sea interface and in DIC, and the DIC deficit at Southern Ocean sites and in iron fertilization experiments

	Month	MLD (m)	$-\Delta fCO_2$(w−a) (μatm)	$-\Delta$DIC (μmol kg^{-1})	DIC deficit (mol m^{-2})	Reference
PFZ, Crozet HP north	11–12	22–85	55 ± 11	60	3.4 ± 0.2[a]	This study
PFZ, Crozet P north	12–01	19–59	42 ± 14	60	2.5 ± 0.1[a]	This study
PFZ, Crozet edge	01	20–33	60	30	3.0 ± 0.1[a]	This study
PFZ, Crozet east	12	104	22 ± 5	20	1.6 ± 0.2[a]	This study
PFZ, Crozet south	01	63, 93	21 ± 2	30	1.3 ± 0.1[a]	This study
PFZ, Crozet Basin, 62°E 45°S	02	50	n.a.	n.a.	1.5 ± 0.2[g]	Leblanc et al. (2002)
PFZ, 170°W 58–60°S	01/03	53/96	50/26	35/30	1.5[d]–2.5[f]/ 2.8[f]	Morrison et al. (2001), Green and Sambrotto (2006)
PF, 170°W 60–61°S	01/03	58/85	69/28	60/45	1.7[d]–2.1[f] / 2.0[f]	Morrison et al. (2001), Green and Sambrotto (2006)
PF, 6°W 47–51°S	11	80	21	7	1.4[e]	Bakker et al. (1997)
MIZ, 140°E 65°S	12–01	10–20	n.a.	70–80	0.9 (0.3–2.5)[c]	Ishii et al. (2002)
SIZ, 30–150°E 64–70°S	02–03	<40–60	n.a.	(120)	2.2 (0.8–4.0)[b]	Ishii et al. (1998)
Prydz Bay, 79°E 68°S	01–03	5	250	600	2.8 (1.3–4.0)[b]	Ishii et al. (1998), Gibson and Trull (1999)
Ross Sea, 169–186°E 77°S	01–02	10–80	80–150	70–150	4.8 (1.2–10.8)[a]	Bates et al. (1998), Sweeney et al. (2000)
Iron addition						
SOFeX_N, 55°S	01–02	40	n.a.	15 ± 2	0.1–1.2[h]	Bishop et al. (2004), Buesseler et al. (2004), Coale et al. (2004)
PFZ, EisenEx, 48°S	11	10–100	18	12	0.7[e]	Bakker et al. (2005)
sACC, SOIREE, 61°S	02	65	38	18	0.8[e]	Bakker et al. (2005)
sACC, SOFeX_S, 66°S	01–02	45	n.a.	16 ± 6	0.1[i]–0.2[h]	Bishop et al. (2004), Buesseler et al. (2004), Coale et al. (2004)

Results are shown for the Crozet Plateau, the Crozet Basin, 170°W, 6°W, the marginal (MIZ) and seasonal ice zones (SIZ) of the Indian Ocean, the Ross Sea and Pryzd Bay. Data are also presented for the SOIREE, EisenEx and SOFeX iron enrichment experiments. Hydrographic regions include the Polar Frontal Zone (PFZ) and the Polar Front (PF). *Notes*: [a]DIC deficit in the upper 100 m, [b]DIC deficit in the summer mixed layer with a depth of 40–60 m (Ishii et al., 1998), [c]DIC deficit relative to the depth with the temperature minimum, [d]DIC deficit from fCO_2 change, [e]net community production (NCP) from fCO_2 change in the mixed layer and other terms, [f]NCP from the DIC deficit in the Ekman layer and other terms, [g]POC surplus in the upper 150 m, [h]POC flux from upper 100 m from an autonomous float, [i]POC flux in upper 100 m from the thorium deficit. 'n.a.' indicates that the value is not available.

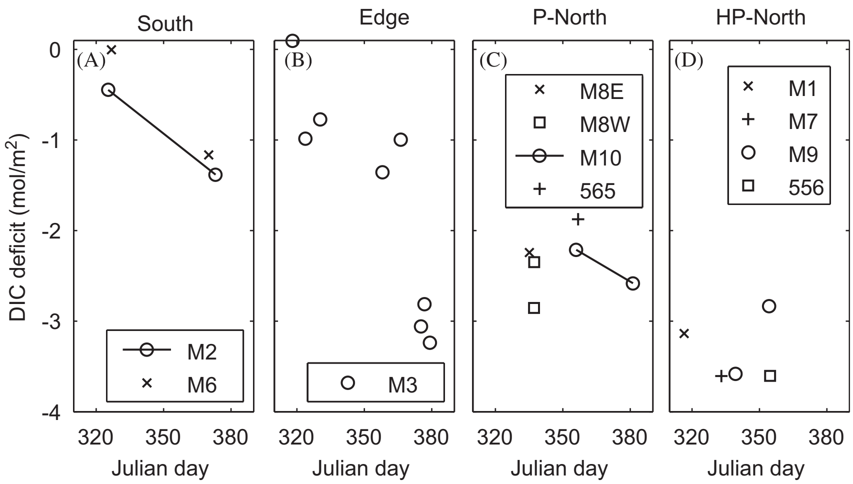

Fig. 7. The evolution of the DIC deficit in the upper 100 m at CTD stations (A) south (upstream) of, (B) on the edge of, (C) in the productive (P) north of, and (D) the highly productive (HP) north of the Crozet Plateau for Julian days in 2004–2005.

where changes in DIC by air–sea transfer and vertical diffusion were equivalent to less than 15% of net community production (Bakker et al., 2006; and references therein). South of the plateau, air–sea gas exchange supplied 18% the DIC deficit during CROZEX (Tables 2a and 2b).

4. Discussion

4.1. The island mass effect for the Crozet Archipelago

The marine cycles of carbon and oxygen differed considerably upstream (south) and downstream (north, edges, east) of the Crozet Plateau in austral spring and summer (Figs. 2–7). Marine productivity was low upstream (south) of the plateau, while extensive phytoplankton blooms strongly reduced DIC and $\Delta f CO_2$(w−a) and increased the O_2 saturation downstream (north, on the edges) of the plateau. Oceanic uptake of atmospheric CO_2 was small upstream of the plateau, while the blooms north of the plateau created an important sink for atmospheric CO_2 (Table 2a). Importantly, the data indicate a difference from upstream to downstream of the plateau in the size and timing of DIC uptake by phytoplankton (Fig. 7):

- *Upstream (south) of the plateau (M2, M6)*: HNLC waters. Little DIC uptake by November. Significant DIC uptake by January.
- *Edge of the plateau (M3)*: Some DIC uptake from November to December. A local phytoplankton bloom with a large DIC deficit in January.
- *Downstream (north) of the plateau I (M10, 15565)*: Productive waters with sizeable DIC uptake in phytoplankton blooms by mid-November.
- *Downstream (north) of the plateau II*: Highly productive waters with extensive phytoplankton blooms at some distance north of the plateau (M1, N1, M9, 15556), as well as northwest of the plateau (M7). Large DIC uptake by November.

These observations confirm the occurrence of an island mass effect for the Crozet Plateau. The island mass effect increased the DIC deficit by a factor 1.9–2.6 downstream of the plateau relative to upstream and created on oceanic CO_2 sink of 1.3 ± 0.8 Tg C downstream of the plateau.

The island mass effect reflects the supply of iron from a source on the Crozet Plateau to waters downstream prior to the bloom event (Planquette et al., 2007). Evidence of iron supply from the island shelf system was found near Ile de la Possession (Planquette et al., 2007). Iron inputs by horizontal advection from the plateau (71%), atmospheric inputs (18%) and vertical mixing (11%) have been estimated to increase the dissolved iron concentration to 0.55 nM in the surface waters of the bloom area by the end of winter (Planquette et al., 2007). The relatively weak currents and the long residence time of the water (60 days) allow a supply of iron to the whole bloom area over the winter period. The iron demand for new production in the bloom region has been independently estimated as 0.75 nM (Lucas et al., 2007). These values compare to an iron concentration upstream (south) of the plateau of roughly 0.17 nM in late winter by iron inputs from atmospheric input and vertical mixing (Planquette et al., 2007).

4.2. North–south gradients in the DIC uptake north of the plateau

The data indicate a latitudinal gradient in the timing of the DIC uptake north of the plateau, where iron supply over the winter period increased the iron concentration to a level favourable for phytoplankton growth (Planquette et al., 2007). In 2004, similar to most years since 1997, the phytoplankton blooms started at some distance north of the plateau, south of the SAF, and spread southwards towards the plateau at an average rate of 4–7 days per degree latitude (Venables et al., 2007). Currents were weak in the bloom area (Pollard et al., 2007), such that horizontal advection of the blooms does not explain this southward progression. Latitudinal differences in the mixed-layer depth and the incoming solar irradiance in spring promoted the north–south gradient in the timing of the phytoplankton blooms (Venables et al., 2007). The most northerly sites (M1, N1) had shallower mixed-layer depths and received higher solar irradiance than those further south (M10), resulting in an earlier start of the blooms and algal DIC uptake further north. Thus, physical conditions controlled the southward progression of the bloom in the iron enriched waters (Venables et al., 2007).

The island mass effect does not explain why regions at some distance north of the plateau (M1, N1) were more productive and had a higher DIC deficit than waters closer to the plateau (M10). The blooms in 2004/2005 were atypical in this respect, as blooms in other years since 1997 had their maximum intensity along the northern edge of the plateau (Venables et al., 2007). A possible explanation is that HNLC water from south of the plateau travelled anticlockwise around the plateau in spring 2004, roughly following the trajectory in Fig. 1B, and reduced phytoplankton productivity just north of the plateau (Venables et al., 2007). Evidence of the advection of HNLC waters from the south was found north of the islands in mid-November (Pollard et al., 2007).

4.3. The HNLC waters upstream of the plateau

Satellite and shipboard surface chlorophyll *a* concentrations suggested low phytoplankton activity at M2 and M6 upstream (south) of the plateau (Fig. 2) (Seeyave et al., 2007). Primary productivity at M2 and M6 was modest, 0.2–0.4 $g\,C\,m^{-2}\,d^{-1}$ in November and January (Seeyave et al., 2007). Phytoplankton uptake reduced the DIC concentration by 15 $\mu mol\,kg^{-1}$, resulting in a significant DIC deficit of $1.3 \pm 0.1\ mol\,m^{-2}$ at the southerly stations in January (Figs. 6 and 7). A reduction of the silicate concentration occurred in parallel (R. Sanders, unpublished results). The O_2 saturation and ΔfCO_2(w−a) were poor indicators of this modest phytoplankton growth, as surface water warming and air–sea gas transfer, counteracted its effects on these parameters.

Circumstantial evidence suggests that M2 and M6 received some inputs of the Crozet Plateau or other shallow topography. Kelp strands were observed at M2 and M6 in January and a few individuals of the neritic copepod *Drepanopus pectinatus* were caught at M2 (Fielding et al., 2007), but contamination of the net cannot be excluded (S. Fielding, personal communication). Much higher numbers of this copepod were found in the vicinity of the Crozet Plateau (Fielding et al., 2007). If the southerly stations received significant inputs from shallow topography, marine productivity at the stations would have been slightly higher than in typical HNLC waters.

In addition, seasonally integrated marine productivity and algal DIC uptake may be higher in the HNLC waters of the PFZ than commonly thought. The DIC deficit at M2 and M6 ($1.3 \pm 0.1\ mol\,m^{-2}$) was similar to the build-up of POC in the upper 150 m in the Crozet Basin (Leblanc et al., 2002) and to the DIC deficit at other sites in the PFZ and at the PF (Table 3). Low, but persistent, marine productivity over a deep mixed layer (133–140 m in November and 63–93 m in January at M2 and M6) (Table 1) may appear unproductive from space and in short time series of shipboard data. An underestimation of surface chlorophyll *a* in ocean colour observations, as seen for CROZEX (Venables et al., 2007), may contribute to the perception of low marine productivity in HNLC waters. Inverse modelling of nutrients suggests that satellite chlorophyll underestimates marine productivity and carbon export south of 50°S (Schlitzer, 2002).

4.4. A Southern Ocean perspective

The Crozet blooms were highly productive blooms in a Southern Ocean context. Only blooms in the Ross Sea, Prydz Bay, and the Seasonal Ice

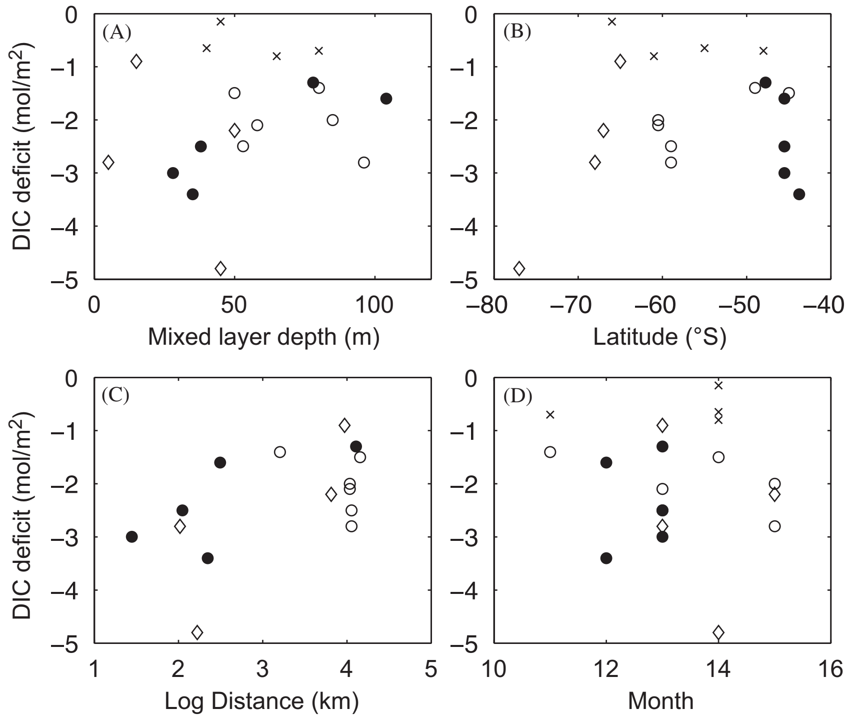

Fig. 8. The DIC deficit (mol m^{-2}) for the Southern Ocean studies in Table 3 as function of (A) mixed-layer depth, (B) latitude, (C) the logarithm of the distance downstream of shallow topography, and (D) month of the year. Symbols indicate the origin of the data: CROZEX (closed circles), other PFZ and PF studies (open circles), studies south of the PF (diamonds), and iron fertilization experiments (crosses). Average values are shown for the DIC deficit in Prydz Bay and the Seasonal Ice Zone. (C) The distance downstream of shallow topography has been crudely estimated, while assuming eastward flow in the Antarctic Circumpolar Current, with exceptions near the Crozet Plateau. (D) Twelve months have been added to months in the first half of the year.

Zone had a higher DIC deficit (Fig. 8; Table 3). Phytoplankton blooms, which developed upon purposeful iron fertilization, had a noticeably lower DIC deficit (0.1–1.2 mol m^{-2}) than natural blooms, which may be explained by the relatively short duration of the iron fertilization experiments.

The DIC deficit in the Southern Ocean studies does not exhibit a clear relationship with, latitude, or month of the year (Fig. 8; Table 3). However, it shows a broad dependence on the distance downstream of land and shallow topography and to a lesser extent with mixed layer depth. Note that this distance downstream has been calculated rather crudely here, while assuming that water in the ACC flows eastward, with exceptions near the Crozet Plateau. The DIC deficit at sites at 10^4 km downstream of shallow topography (e.g. along 170°W) (0.9–2.2 mol C m^{-2}) is a third to half of that at sites within 500 km from land (2.5–4.8 mol C m^{-2}). The DIC deficit upstream (south) of the Crozet Plateau (1.3 mol C m^{-2}) fits well with values at sites 10^4 km downstream of land.

5. Conclusions

The island mass effect has been quantified for inorganic carbon changes and CO_2 air–sea fluxes in waters near the Crozet Plateau for November 2004 to January 2005. The maximum DIC deficit in the upper 100 m ranged from 3.4 ± 0.2 mol m^{-2} in the highly productive waters downstream (north) of the plateau to 1.3 ± 0.1 mol m^{-2} upstream (south) of the plateau (Fig. 7; Table 2b). Extensive phytoplankton blooms downstream (north) of the plateau created an oceanic CO_2 sink of 1.3 ± 0.8 Tg C during CROZEX. The island mass effect reflects differences in the supply of iron to these waters (Planquette et al., 2007). A north–south gradient in the timing of algal DIC uptake north of the plateau is explained by latitudinal differences in the mixed-layer depth and in incoming solar irradiance (Venables et al., 2007). The DIC deficit in the HNLC waters upstream (south) of the plateau was a third to half of that in the highly productive waters downstream (north) of the plateau, suggesting that

HNLC waters of the PFZ are more productive than commonly thought. The Crozet blooms are among the most productive blooms studied in the Southern Ocean.

The DIC deficit in phytoplankton blooms upon purposeful iron fertilization is considerably lower than in natural blooms and in HNLC waters, suggesting that relatively short studies of artificial iron fertilized blooms are not perfect analogues for the natural world. The DIC deficit at Southern Ocean sites shows a broad dependence on the distance downstream of shallow topography and to a lesser extent with mixed layer depth. The factors controlling phytoplankton growth and DIC uptake in the Southern Ocean are complex. Time-series studies at key sites, encompassing at least one growing season and a winter season, are essential for a better understanding of marine carbon and oxygen cycling in the Southern Ocean. Studies in the vast expanse of subantarctic HNLC waters are particularly important (Banse, 1996, 2004).

Acknowledgements

The captain and crew of *RRS Discovery* and *UKORS* (United Kingdom Ocean Research Services) staff enthusiastically supported the CROZEX cruises. Raymond Pollard, Richard Sanders, and other scientists on board created an exciting research environment. Comments by Nicolas Metzl and two anonymous reviewers substantially improved this article. The cruises were part of the NERC (Natural Environment Research Council) BICEP (Biophysical Interactions and Controls on Export Production) Core Strategic Project of the George Deacon Division at NOCS. The work was supported by these grants: NERC CASIX (Centre for Observations of Air–Sea Interactions and Fluxes, NER/F14/G6/115), EU CARBOOCEAN (GOCE-511176-1) and the NERC LGMAC (Laboratory for Global Marine and Atmospheric Chemistry) Joint Infrastructure Fund (NER/H/S/1999/00176).

References

Aanderaa, 2003. Operating Manual Oxygen Optode 3830 and 3930, ninth ed. Technical Document 218. Aanderaa Instruments AS, Bergen, Norway.

Antoine, D., André, J-M., Morel, A., 1996. Oceanic primary production. 2. Estimation at global scale from satellite (coastal zone color scanner) chlorophyll. Global Biogeochemical Cycles 10, 57–69.

Bakker, D.C.E., de Baar, H.J.W., Bathmann, U.V., 1997. Changes of carbon dioxide in surface waters during spring in the Southern Ocean. Deep-Sea Research Part II 44, 91–128.

Bakker, D.C.E., Watson, A.J., Law, C.S., 2001. Southern Ocean iron enrichment promotes inorganic carbon drawdown. Deep-Sea Research Part II 48, 2483–2507.

Bakker, D.C.E., Bozec, Y., Nightingale, P.D., Goldson, L.E., Messias, M.J., de Baar, H.J.W., Liddicoat, M.I., Skjelvan, I., Strass, V., Watson, A.J., 2005. Iron and mixing affect biological carbon uptake in SOIREE and EisenEx, two Southern Ocean iron fertilisation experiments. Deep-Sea Research Part I 52, 1001–1019.

Bakker, D.C.E., Boyd, P.W., Charette, M.A., Hall, J.A., Nodder, S.D., Safi, K., Singleton, R.J., Trull, T.W., Waite, A.M., Watson, A.J., Zeldis, J., Abraham, E.R., Law, C.S., Tanneberger, K., 2006. Matching carbon pools and fluxes for the Southern Ocean Iron Release Experiment (SOIREE). Deep-Sea Research Part I 53, 1941–1960.

Banse, K., 1996. Low seasonality of low concentrations of surface chlorophyll in the Subantarctic water ring: underwater irradiance, iron, or grazing? Progress in Oceanography 37, 241–291.

Banse, K., 2004. Open questions after JGOFS: winter chlorophyll levels in the two subpolar HNLC regions. US JGOFS Letter 12, 14.

Bates, N.R., Hansell, D.A., Carlson, C.A., 1998. Distribution of CO_2 species, estimates of net community production, and air–sea CO_2 exchange in the Ross Sea polynia. Journal of Geophysical Research 103, 2883–2896.

Behrenfeld, M.J., Falkowski, P.G., 1997. Photosynthetic rates derived from satellite-based chlorophyll concentration. Limnology and Oceanography 42, 1–20.

Bishop, J.K., Wood, T.J., Davis, R.E., Sherman, J.T., 2004. Robotic observations of enhanced carbon biomass and export at 55°S during SOFeX. Science 304, 417–420.

Boyd, P.W., LaRoche, J., Gall, M., Frew, R., McKay, R.M.L., 1999. Role of iron, light and silicate in controlling algal biomass in subantarctic waters SE of New Zealand. Journal of Geophysical Research 104, 13395–13408.

Brainerd, K.E., Gregg, M.C., 1995. Surface mixed and mixing layer depths. Deep-Sea Research Part I 42, 1521–1543.

Broecker, W.S., Peng, T.H., 1982. Tracers in the Sea. Eldigio Press, Columbia University, Palisades, New York.

Bucciarelli, E., Blain, S., Tréguer, P., 2001. Iron and manganese in the wake of the Kerguelen Islands (Southern Ocean). Marine Chemistry 73, 21–36.

Buesseler, K.O., Andrew, J., Pike, S., Charette, M.A., 2004. The effects of iron fertilization on carbon sequestration in the Southern Ocean. Science 304, 414–417.

Caldeira, K., Duffy, P.B., 2000. The role of the Southern Ocean in uptake and storage of anthropogenic carbon dioxide. Science 287, 620–622.

Coale, K.H., Johnson, K.S., Chavez, F.P., Buesseler, K.O., Barber, R.T., Brzezinski, M.A., Cochlan, W.P., Millero, F.J., Falkowski, P.G., Bauer, J.E., Wanninkhof, R.H., Kudela, R.M., Altabet, M.A., Hales, B.E., Takahashi, T., Landry, M.R., Bidigare, R.R., Wang, X., Chase, Z., Strutton, P.G., Friederich, G.E., Gorbunov, M.Y., Lance, V.P., Hilting, A.K., Hiscock, M.R., Demarest, M., Hiscock, W.T., Sullivan, K.F., Tanner, S.J., Gordon, R.M., Hunter, C.N., Elrod, V.A., Fitzwater, S.E., Jones, J.L., Tozzi, S., Koblizek, M., Roberts, A.E., Herndon, J., Brewster, J., Ladizinsky, N., Smith, G., Cooper, D., Timothy, D., Brown, S.L., Selph, K.E., Sheridan, C.C., Twining, B.S., Johnson, Z.I., 2004. Southern Ocean iron enrichment experiment: carbon cycling in high- and low-Si waters. Science 304, 408–414.

de Baar, H.J.W., de Jong, J.T.M., Bakker, D.C.E., Löscher, B.M., Veth, C., Bathmann, U.V., Smetacek, V., 1995. Importance of iron for plankton blooms and carbon dioxide drawdown in the Southern Ocean. Nature 373, 412–415.

DOE, 1994. In: Dickson, A.G., Goyet, C. (Eds.), Handbook of Methods for the Analysis of the Various Parameters of the Carbon System in Sea Water; version 2. ORNL/CDIAC 74.

Doty, M.S., Oguri, M., 1956. The island mass effect. Journal du Conseil Permanent International de la Exploration de la Mer 22, 33–37.

Fielding, S., Ward, P., Pollard, R.T., Seeyave, S., Read, J.F., Hughes, J.A., Smith, T., Castellini, C., 2007. Community structure and grazing impact of mesozooplankton during late spring/early summer 2004/2005 in the vicinity of the Crozet Islands (Southern Ocean). Deep-Sea Research Part II, this issue [doi:10.1016/j.dsr2.2007.06.016].

Garcia, H.E., Gordon, L.I., 1992. Oxygen solubility in seawater: better fitting equations. Limnology and Oceanography 37, 1307–1312.

Gervais, F., Riebesell, U., Gorbunov, M.Y., 2002. Changes in the size-fractionated primary productivity and *chlorophyll a* in response to iron fertilization in the southern Polar Frontal Zone. Limnology and Oceanography 47, 1324–1335.

Gibson, J.A.E., Trull, T.W., 1999. Annual cycle of fCO_2 under sea-ice and in open water in Prydz Bay, East Antarctica. Marine Chemistry 66, 187–200.

Gilmartin, M., Revelante, N., 1974. The 'island mass' effect on the phytoplankton and primary production of the Hawaiian islands. Journal of Experimental Marine Biology and Ecology 16, 181–204.

Green, S.E., Sambrotto, R.N., 2006. Net community production in terms of C, N, P and Si in the Antarctic Circumpolar Current and its influence on regional water mass characteristics. Deep-Sea Research Part I 53, 111–135.

Gurney, K.R., Law, R.M., Denning, A.S., Rayner, P.J., Baker, D., Bousquet, P., Bruhwiler, L., Chen, Y.-H., Ciais, P., Fan, S., Fung, I.Y., Gloor, M., Heimann, M., Higuchi, K., John, J., Maki, T., Maksyutov, S., Masarie, K., Peylin, P., Prather, M., Pak, B.C., Randerson, J., Sarmiento, J., Taguchi, S., Takahashi, T., Yuen, C.-W., 2002. Towards robust regional estimates of CO_2 sources and sinks using atmospheric transport models. Nature 415, 626–630.

Ishii, M., Inoue, H.Y., Matsueda, H., Tanoue, E., 1998. Close coupling between seasonal biological production and dynamics of dissolved inorganic carbon in the Indian Ocean sector and the western Pacific Ocean sector of the Antarctic Ocean. Deep-Sea Research Part I 45, 1187–1209.

Ishii, M., Inoue, H.Y., Matsueda, H., 2002. Net community production in the marginal ice zone and its importance for the variability of oceanic pCO_2 in the Southern Ocean south of Australia. Deep-Sea Research Part II 49, 1691–1706.

Johnson, K.M., Williams, P.J.LeB., Brändström, L., Sieburth, J.McN., 1987. Coulometric total carbon dioxide analysis for marine studies: automatization and calibration. Marine Chemistry 21, 117–133.

Korb, R.E., Whitehouse, M.J., Ward, P., 2004. SeaWiFS in the southern ocean: spatial and temporal variability in phytoplankton biomass around South Georgia. Deep-Sea Research Part II 51, 99–116.

Large, W.G., Pond, S., 1981. Open ocean momentum flux measurements in moderate to strong winds. Journal of Physical Oceanography 11, 324–336.

Leblanc, K., Quéguiner, B., Fiala, M., Blain, S., Morvan, J., Corvaisier, 2002. Particulate biogenic silica and carbon production rates and particulate matter distribution in the Indian sector of the Subantarctic Ocean. Deep-Sea Research Part II 49, 3189–3206.

Lucas, M., Seeyave, S., Sanders, R., Moore, C.M., Williamson, R., Stinchcombe, M., 2007. Nitrogen uptake responses to a naturally Fe-fertilised phytoplankton bloom during the 2004/5 CROZEX study. Deep-Sea Research Part II, this issue [doi:10.1016/j.dsr2.2007.06.017].

Lo Monaco, C., Goyet, C., Metzl, N., Poisson, A., Touratier, F., 2005. Distribution and inventory of anthropogenic CO_2 in the Southern Ocean: comparison of three data-based methods. Journal of Geophysical Research 110 (C09S02), 1–12.

Metzl, N., Brunet, C., Jabaud-Jan, A., Poisson, A., Schauer, B., 2006. Summer and winter air–sea CO_2 fluxes in the Southern Ocean. Deep-Sea Research Part I 53, 1548–1563.

Moore, J.K., Abbott, M.R., 2000. Phytoplankton chlorophyll distributions and primary production in the Southern Ocean. Journal of Geophysical Research 105, 28709–28722.

Moore, J.K., Abbott, M.R., 2002. Surface chlorophyll concentrations in relation to the Antarctic Polar Front: seasonal and spatial patterns from satellite observations. Journal of Marine Systems 37, 69–86.

Morrison, J.M., Gaurin, S., Codispoti, L.A., Takahashi, T., Millero, F.J., Gardner, W.D., Richardson, M.J., 2001. Seasonal evolution of hydrographic properties in the Antarctic Circumpolar Current at 170°W during 1997–1998. Deep-Sea Research Part II 48, 3943–3972.

Nelson, D.M., Smith Jr., W.O., 1991. Sverdrup revisited: critical depths, maximum chlorophyll levels, and the control of Southern Ocean productivity by the irradiance-mixing regime. Limnology and Oceanography 36, 1650–1661.

Nelson, D.M., Anderson, R.F., Barber, R.T., Brzezinski, M.A., Buesseler, K.O., Chase, Z., Collier, R.W., Dickson, M.-L., François, R., Hiscock, M.R., Honjo, S., Marra, J., Martin, W.R., Sambrotto, R.N., Sayles, F.L., Sigmon, D.E., 2002. Vertical budgets for organic carbon and biogenic silica in the Pacific sector of the Southern Ocean, 1996–1998. Deep-Sea Research Part II 49, 1645–1674.

Orsi, A.H., Whitworth III, T., Nowling Jr., W.D., 1995. On the meridional extent and fronts of the Antarctic Circumpolar Current. Deep-Sea Research Part I 42, 641–673.

Peylin, P., Bousquet, P., Le Quéré, C., Sitch, S., Friedlingstein, P., McKinley, G., Gruber, N., Rayner, P., Ciais, P., 2005. Multiple constraints on regional CO_2 flux variations over land and oceans. Global Biogeochemical Cycles 19 (GB1011), 1–21.

Planquette, H., Statham, P.J., Fones, G.R., Charette, M.A., Moore, M., Salter, I., Nédélec, F.H., Taylor, S.L., French, M., Baker, A.R., Mahowald, N., Jickells, T.D., 2007. Dissolved iron in the vicinity of the Crozet Islands, Southern Ocean. Deep-Sea Research Part II, this issue [doi:10.1016/j.dsr2.2007.06.019].

Platt, T., Broomhead, D.S., Sathyendranath, S., Edwards, A.M., Murphy, E., 2003. Phytoplankton biomass and residual nitrate in the pelagic ecosystem. Proceedings of the Royal Society of London A 459, 1063–1073.

Pollard, R.T., Reid, J.F., 2001. Circulation pathways and transports of the Southern Ocean in the vicinity of the Southwest Indian Ridge. Journal of Geophysical Research 106, 2881–2898.

Pollard, R.T., Lucas, M.I., Read, J.F., 2002. Physical controls on biogeochemical zonation in the Southern Ocean. Deep-Sea Research Part II 49, 3289–3305.

Pollard, R.T., Venables, H.J., Read, J.F., Allen, J.T., 2007. Large scale circulation around the Crozet Plateau controls an annual phytoplankton bloom in the Crozet Basin. Deep-Sea Research Part II, this issue [doi:10.1016/j.dsr2.2007.06.012].

Rayner, P.J., Enting, I.G., Francey, R.J., Langenfelds, R., 1999. Reconstructing the recent carbon cycle from atmospheric CO_2, $\delta^{13}C$ and O_2/N_2 observations. Tellus 51B, 213–232.

Rintoul, S.R., Hughes, C.W., Olbers, D., 2001. The Antarctic Circumpolar current system. In: Siedler, G., Church, J., Gould J. (Eds.), Ocean Circulation and Climate. International Geophysics Series 77, pp. 271–302.

Sabine, C.L., Feely, R.A., Gruber, N., Key, R.M., Lee, K., Bullister, J.L., Wanninkhof, R., Wong, C.S., Wallace, D.W.R., Tilbrook, B., Millero, F.J., Peng, T.H., Kozyr, A., Ono T., RiosA.F., 2004. The oceanic sink for anthropogenic CO_2. Science 305, 367–371.

Sanders, R., Morris, P.J., Stinchcombe, M., Seeyave, S., Venables, H.J., Lucas, M., Moore, M., 2007. New production and the *f*-ratio around the Crozet Plateau in austral summer 2004-5 diagnosed from seasonal changes in inorganic nutrient levels. Deep-Sea Research Part II, this issue [doi:10.1016/j.dsr2.2007.06.007].

Schlitzer, R., 2002. Carbon export fluxes in the Southern Ocean: results from inverse modelling and comparison with satellite-based estimates. Deep-Sea Research Part II 49, 1623–1644.

Schuster, U., Watson, A.J., 2007. A variable and decreasing sink for atmospheric CO_2 in the North Atlantic. Journal of Geophysical Research, accepted.

Seeyave, S., Lucas, M.I., Moore, C.M., Poulton, A.J., 2007. Phytoplankton productivity and community structure in the vicinity of the Crozet Plateau during austral summer 2004/2005. Deep-Sea Research Part II, this issue [doi:10.1016/j.dsr2.2007.06.010].

Smith, W.H.F., Sandwell, D.T., 1997. Global seafloor topography from satellite altimetry and ship depth soundings. Science 277, 1956–1962.

Speer, K., Rintoul, S.R., Sloyan, B., 2000. The diabatic Deacon cell. Journal of Physical Oceanography 30, 3212–3222.

Sullivan, C.W., Arrigo, K.R., McClain, C.R., Comiso, J.C., Firestone, J., 1993. Distributions of phytoplankton blooms in the Southern Ocean. Science 262, 1832–1837.

Sunda, W.G., Huntsman, S.A., 1997. Interrelated influence of iron, light and cell size on marine phytoplankton growth. Nature 390, 389–392.

Sweeney, C., Hansell, D.A., Carlson, C.A., Codispoti, L.A., Gordon, L.I., Marra, J., Millero, F.J., Smith, W.O., Takahashi, T., 2000. Biological regimes, net community production and carbon export in the Ross Sea, Antarctica. Deep-Sea Research Part II 47, 3369–3394.

Takahashi, T., Olafsson, J., Goddard, J.G., Chipman, D.W., Sutherland, S.C., 1993. Seasonal variation of CO_2 and nutrients in the high-latitude surface oceans: a comparative study. Global Biogeochemical Cycles 7, 843–878.

Takahashi, T., Sutherland, S.C., Sweeney, C., Poisson, A., Metzl, N., Tilbrook, B., Bates, N., Wanninkhof, R.H., Feely, R.A., Sabine, C., Olafsson, J., Nojiri, Y., 2002. Global sea–air CO_2 flux based on climatological surface ocean pCO_2, and seasonal biological and temperature effects. Deep-Sea Research Part II 49, 1601–1622.

Tyrrell, T., Merico, A., Waniek, J.J., Wong, C.S., Metzl, N., Whitney, F., 2005. Effect of seafloor depth on phytoplankton blooms in high-nitrate, low-chlorophyll (HNLC) regions. Journal of Geophysical Research 110 (G02006), 1–12.

Venables, H.J., Pollard, R.T., Popova, E.E., 2007. Physical conditions controlling the early development of a regular phytoplankton bloom north of the Crozet Plateau, Southern Ocean, described using remotely sensed data. Deep-Sea Research Part II, this issue [doi:10.1016/j.dsr2.2007.06.014].

Wanninkhof, R.H., 1992. Relationship between wind speed and gas exchange over the ocean. Journal of Geophysical Research 97, 7373–7382.

Weiss, R.F., Price, B.A., 1980. Nitrous oxide solubility in water and seawater. Marine Chemistry 8, 347–359.

Williams, P.J.leB., Morris, P.J., Karl, D., 2004. Net community production and metabolic balance at the oligotrophic ocean site, station ALOHA. Deep-Sea Research Part I 51, 1563–1578.